OXFORD

JNCI J Natl Cancer Inst (2019) 111(6): djy150

doi: 10.1093/jnci/djy150
First published online October 8, 2018
Article

ARTICLE

Genome-Wide Association Study of Susceptibility Loci for Radiation-Induced Brain Injury

Tong-Min Wang*, Guo-Ping Shen*, Ming-Yuan Chen*, Jiang-Bo Zhang*, Ying Sun*, Jing He, Wen-Qiong Xue, Xi-Zhao Li, Shao-Yi Huang, Xiao-Hui Zheng, Shao-Dan Zhang, Ye-Zhu Hu, Hai-De Qin, Jin-Xin Bei, Jun Ma, Jianbing Mu, Yin Yao Shugart, Wei-Hua Jia

See the Notes section for the full list of authors' affiliations.

*These authors contributed equally to this work.

Correspondence to: Wei-Hua Jia, PhD, State Key Laboratory of Oncology in South China, Collaborative Innovation Center for Cancer Medicine, Guangdong Key Laboratory of Nasopharyngeal Carcinoma Diagnosis and Therapy, Sun Yat-sen University Cancer Center, Guangzhou 510060, China (e-mail: jiawh@sysucc.org.cn).

Abstract

Background: Radiation-induced brain injury is a nonnegligible issue in the management of cancer patients treated by partial or whole brain irradiation. In particular, temporal lobe injury (TLI), a deleterious late complication in nasopharyngeal carcinoma, greatly affects the long-term life quality of these patients. Although genome-wide association studies (GWASs) have successfully identified single nucleotide polymorphisms (SNPs) associated with radiation toxicity, genetic variants contributing to the radiation-induced brain injury have not yet been assessed.
Methods: We recruited and performed follow-up for a prospective observational cohort, Genetic Architecture of Radiotherapy Toxicity and Prognosis, using magnetic resonance imaging for TLI diagnosis. We conducted genome-wide association analysis in 1082 patients and validated the top associations in two independent cohorts of 1119 and 741 patients, respectively. All statistical tests were two-sided.
Results: We identified a promoter variant rs17111237 (A > G, minor allele frequency [MAF] = 0.14) in *CEP128* associated with TLI risk (hazard ratio = 1.45, 95% confidence interval = 1.26 to 1.66, $P_{combined}=3.18\times10^{-7}$) which is in moderate linkage disequilibrium (LD) with rs162171 (MAF = 0.18, $R^2 = 0.69$), the top signal in *CEP128* (hazard ratio = 1.46, 95% confidence interval = 1.29–1.66, $P_{combined} = 6.17\times10^{-9}$). Combining the clinical variables with the top SNP, we divided the patients into different subgroups with varying risk with 5-year TLI-free rates ranging from 33.7% to 95.5%. *CEP128*, a key component of mother centriole, tightly interacts with multiple radiation-resistant genes and plays an important role in maintaining the functional cilia, which otherwise will lead to a malfunction of the neural network. We found that A > G alteration at rs17111237 impaired the promoter activity of *CEP128* and knockdown of *CEP128* decreased the clonogenic cell survival of U87 cells under radiation. Noteworthy, 12.7% (27/212) of the GWAS-based associated genes ($P < .001$) were enriched in the neurogenesis pathway.
Conclusions: This three-stage study is the first GWAS of radiation-induced brain injury that implicates the genetic susceptibility gene *CEP128* involved in TLI development and provides the novel insight into the underlying mechanisms of radiation-induced brain injury.

Radiation-induced brain injury is an important issue in the management of cancer patients treated by partial or whole-brain irradiation, which were characterized from mild fatigue to neurocognitive deficits such as progressive memory difficulties and even death (1). Many confounding factors including short life spans and tumor effects on the brain have posed great

Received: January 16, 2018; **Revised:** May 24, 2018; **Accepted:** July 29, 2018

challenges for the discovery of reliable biomarkers to predict radiation-susceptible patients and for the disclosure of the mechanism of radiation-induced brain injury. Temporal lobe injury (TLI), a deleterious late radiotherapy toxicity of nasopharyngeal carcinoma (NPC) (2,3) resulting from unavoidable radiation exposure of the inferior and medial aspects of temporal lobes, however, provides several unique conditions for such study, including no direct effects of brain tumors, longer survival of patients, and distinct phenotypic characterization. Although intensity-modulated radiotherapy (IMRT) with more controlled dose deposition in normal tissue has reduced the rate of TLI, there are still 3.2–12.9% of NPC survivors suffering TLI in months to years postradiotherapy (4–9). The TLI symptoms including dizziness, headache, memory impairment, and neurocognitive dysfunctions (10), varied among the patients, often irreversible and that negatively influence the patients' quality of life.

Some clinical parameters including treatment protocols (11) and tumor stages (4) are risk factors of TLI development in NPC patients. However, even after these factors are adjusted, interpatient variability of TLI could not been fully explained, indicating a possible role of a genetic contribution at the individual-level radiosensitivity. Many genetic studies of radiation-induced adverse responses focused on candidate genes involved in DNA repair, DNA damage signaling, cell cycle control, and inflammatory response but many of them had limited sample sizes and suffered a lack of independent replication (12–15). Although several recent genome-wide association studies (GWAS) (16–21) have successfully identified single nucleotide polymorphisms (SNPs) associated with radiation toxicity in patients with prostate and/or breast cancer, the genetic impact of radiation-induced TLI is yet to be reported. Therefore, we initiated a prospective observational clinical trial, GARTP (Genetic Architecture of the Radiotherapy Toxicity and Prognosis) to identify the susceptibility genes contributing to TLI development.

Materials and Methods

The GARTP Study

The GARTP study (registered with www.chictr.org.cn/, ChiCTR-ROC-17012658) is a prospective observational clinical trial that aims to identify the susceptibility genes contributing to recurrence, metastasis, and radiation-induced normal tissue injury in NPC patients. This study was approved by the Human Ethics Approval Committee of Sun Yat-sen University Cancer Center (SYSUCC) on June 15, 2005 (No. YB2005001). The recruitment criteria are described in the Supplementary Methods (available online). All patients agreed to participate in this study and provided written informed consent.

Study Subjects

To focus on the TLI incidence, which is one of the primary endpoints of the GARTP study, we further excluded the patients who did not come back for magnetic resonance imaging (MRI) follow-up after radiotherapy. Between 2005 and 2007, 1166 NPC patients from the GARTP cohort were screened for eligibility for the study of TLI development. After pretreatment evaluation, we followed up the MRI of nasopharynx/brain of all but 84 patients who did not return for MRI follow-up after radiotherapy. The detailed information of study design is shown in Figure 1. We included a total of 1082 NPC patients in the discovery stage. All the patients were staged according to the 2002 6th UICC/AJCC staging system (22). Radiation therapy (two-dimensional conformal, 2D-CRT or IMRT) was used alone or in combination with chemotherapy (Supplementary Methods, available online).

The patients in the first replication stage came from 1164 NPC patients who were recruited from the GARTP study in 2008–2010. Forty-five patients did not return for MRI follow-up after radiotherapy. Therefore, a total of 1119 patients were included in the first replication stage. For the second replication stage, we included 408 NPC patients who were also recruited in the GARTP study in 2005–2007 but were not included in the GWAS analysis. In order to enlarge the sample size, we additionally included 511 patients in 2002–2004 using the same inclusion criteria. After excluding 72 patients in 2005–2007 and 106 patients in 2002–2004 without MRI follow-up after radiotherapy, 741 patients remained in this stage. All the patients received similar dosage prescriptions and used the same UICC/AJCC staging system as those in the discovery stage.

Follow-up and Diagnosis for TLI

After completing therapy, the patients were followed up by MRI of the nasopharynx and/or neck regularly (maximum follow-up time of 15.0 years). We defined the time of TLI development as the time between the date of commencement of the primary radiotherapy and the time when TLI occurred. For patients who had not developed TLI before the end of the study (December 31, 2016), the end times were defined as the last MRI follow-up. For the patients who were treated with a second course of radiotherapy due to local recurrence, their times were defined as the duration between the beginning of the primary radiotherapy and the beginning of the second radiotherapy.

MRI was used for the diagnosis of TLI as previously described (3,4,23) (Supplementary Figure 1, available online). The radiologists and clinical radiation oncologists specializing in head-and-neck cancers evaluated the MR images independently. Any disagreement was resolved by consensus.

DNA Extraction, Genotyping, Imputation, and Quality Control

Detailed description of DNA extraction, genotyping, imputation, and quality control is shown in the Supplementary Methods (available online) and Supplementary Table 1 (available online).

Cell Lines, Constructs, and Functional Assays

For a full description of the laboratory experiments, please see the Supplementary Methods (available online). Human glioblastoma U87 cell line and 293 T cell lines were purchased from the American Type Culture Collection (Manassas, VA) and were cultured in RPMI-1640 or Dulbecco's modified Eagle's medium (DMEM) supplemented with 10.0% fetal bovine serum (FBS, GIBCO, Carlsbad, CA). All cell lines were maintained in a humidified incubator containing 5.0% CO_2 at 37.0°C. For the radiation treatments, cells were irradiated with 6-MV X-rays from a Primus linear accelerator (Siemens, Malvern, PA) with a dose rate of 198 cGy/min.

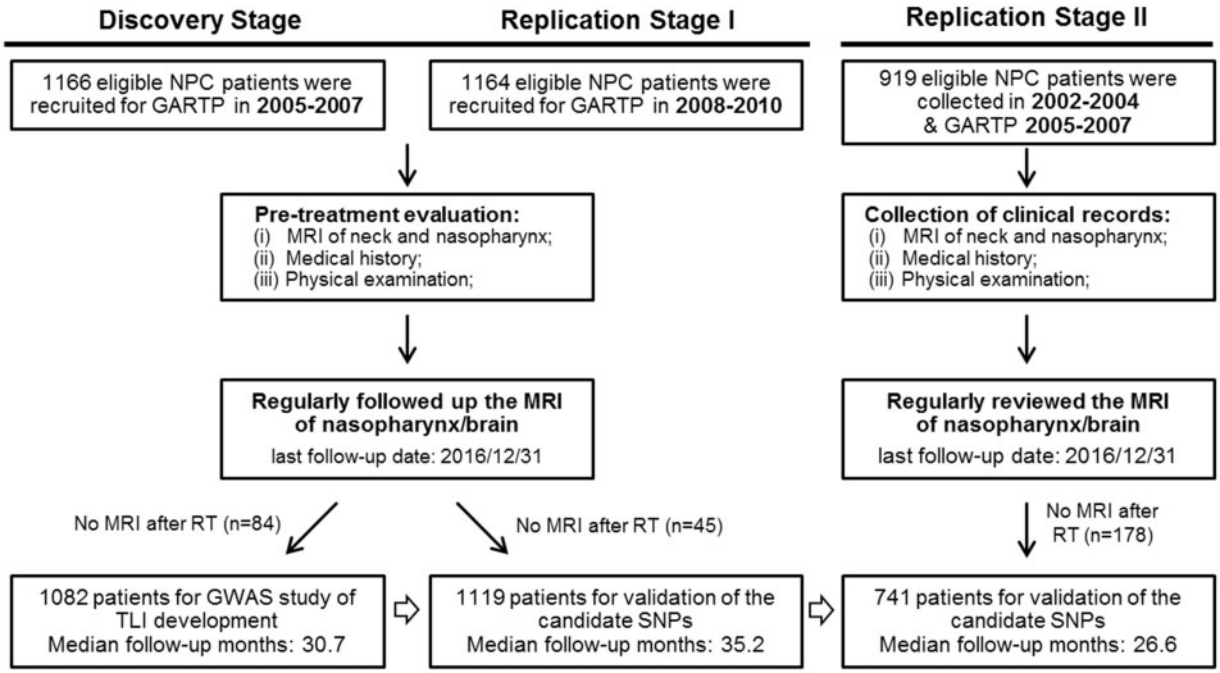

Figure 1. The flow diagram of the study design. NPC = nasopharyngeal carcinoma; GARTP = Genetic Architecture of the Radiotherapy Toxicity and Prognosis; SNP = single nucleotide polymorphism; GWAS = genome-wide association study; TLI = temporal lobe injury; MRI = magnetic resonance imaging; RT = radiotherapy.

Statistical Analysis

All the analysis procedures are shown in Supplementary Figure 2 (available online). GWAS was performed using Cox proportional hazard regression model (24) assuming additive SNP effect. The proportional hazard assumption was verified using Schoenfeld residuals. Two reported risk factors, tumor stage (T stage) and the radiation technique (IMRT or 2D-CRT) (4), as well as age at NPC diagnosis, were adjusted as covariates. Per allele hazard ratios and their 95% confidence intervals [CIs] were estimated using the R package "survival" and the adjusted survival curves were estimated by the R package "survminer." In the discovery stage, SNPs with two-sided P less than 1.0×10^{-5} were selected for validation. A quantile–quantile plot was used to evaluate the overall statistical significance of the GWAS and the deviation of observed vs expected distribution of P values was represented by inflation factor (λ_{GC}) (25). Linkage disequilibrium (LD) between SNPs was calculated with the Haploview program (v. 4.1). The survival tree was constructed by using recursive partitioning under conditional inference framework using the R package "party." For the stopping criterion, Bonferroni correction was used and the level of statistical significance was chosen as .01. We also restricted the maximum depth of the tree to three. A two-sided t-test was used to test the statistical significance between cell survival fractions of control and different shRNAs of *CEP128*. Statistical significance was defined as P less than .05. Pathway/gene set analysis and expression quantitative trait locus (eQTL) analysis is described in the Supplementary Methods (available online). All statistical tests were two-sided.

Results

We included 1082 NPC patients in the discovery stage (Figure 1) and the detailed clinical characteristics are shown in Table 1. The average MRI follow-up was 4.10 times and the median follow-up months were 30.7. Among 1082 patients, 243 (22.5%) developed TLI after radiotherapy. Tumor stage and radiation techniques have been reported to be associated with TLI risk in a previous study (4) and in this clinical trial we confirmed the results. The patients treated with IMRT had a lower TLI incidence, with a hazard ratio (HR) of 0.42 (95% CI = 0.28 to 0.64) compared with those treated by 2D-CRT. Patients with advanced tumor stage exhibited elevated TLI risks with HRs of 2.86 (T2 vs T1, 95% CI = 1.13 to 7.19), 4.30 (T3 vs T1, 95% CI = 1.74 to 10.63), and 7.65 (T4 vs T1, 95% CI = 3.05 to 19.21), respectively (Table 1). Additionally, we found that older people were more likely to develop TLI, with HRs of 1.54 (95% CI = 0.84 to 2.83), 2.08 (95% CI = 1.16 to 3.74), 2.31 (95% CI = 1.28 to 4.18), and 1.67 (95% CI = 0.77 to 3.65) for those in age groups of 31–40 years, 41–50 years, 51–60 years, and 61 years and older, compared with those age 30 years or younger, respectively (Table 1).

After quality controls, 445 078 autosomal SNPs were included in the genome-wide association analysis under an additive assumption using a Cox proportional hazard model (24,26), adjusting age at NPC diagnosis, radiation techniques, and tumor stages, following radiogenomics reporting guidelines (27). The distribution of observed vs expected P values are shown in the quantile–quantile plot with $\lambda_{GC} = 1.00$ (Supplementary Figure 3, available online). We identified seven potentially statistically significant association signals with P values smaller than 1.0×10^{-5} (Figure 2A and Supplementary Table 2, available online). Three of them were located at the introns of *CEP128* with high linkage disequilibrium (LD) ($R^2 = 0.97$–1.00) and the signal could be represented by rs162171 with HR of the minor allele of 1.66 (minor allele frequency [MAF] = 0.17; 95% CI = 1.33 to 2.07) and $P = 7.75 \times 10^{-6}$ (Table 2). Additionally, two intron SNPs of *KCTD1* and one at *DISC1FP1* were associated with TLI risk at a similar statistical significance level.

We then fine mapped 100 kb regions upstream/downstream of *CEP128*, *KCTD1*, and *DISC1FP1* by imputation (28) analysis. We searched the potential functional SNPs with P less than .001 in these regions and found three variants located at the promoter

ARTICLE

Table 1. Characteristics and multivariable regression analysis of temporal lobe injury development in the discovery and replication stages

Characteristics	Discovery stage		Replication stage I		Replication stage II		Combined	
	TLI/ non-TLI	Adjusted HR* (95% CI)	TLI/ non-TLI	Adjusted HR* (95% CI)	TLI/ non-TLI	Adjusted HR* (95% CI)	TLI/non-TLI	Adjusted HR* (95% CI)
Number of patients	243/839	—	261/858	—	177/564	—	681/2261	—
Age, y								
≤30	13/68	1.00 (reference)	16/74	1.00 (reference)	8/49	1.00 (reference)	37/191	1.00 (reference)
31-40	56/241	1.54 (0.84 to 2.83)	69/240	1.73 (1.00 to 2.99)	55/166	2.10 (0.99 to 4.46)	180/647	1.73 (1.22 to 2.47)
41-50	85/256	2.08 (1.16 to 3.74)	84/278	2.23 (1.30 to 3.82)	70/172	2.75 (1.31 to 5.79)	239/706	2.25 (1.59 to 3.18)
51-60	76/181	2.31 (1.28 to 4.18)	71/189	3.05 (1.76 to 5.29)	34/113	2.82 (1.29 to 6.18)	181/483	2.61 (1.83 to 3.72)
≥61	13/93	1.67 (0.77 to 3.65)	21/77	3.12 (1.62 to 6.04)	10/64	2.36 (0.91 to 6.12)	44/234	2.33 (1.50 to 3.62)
Sex								
Male	186/606	1.00 (reference)	200/660	1.00 (reference)	132/436	1.00 (reference)	518/1702	1.00 (reference)
Female	57/233	0.78 (0.58 to 1.06)	61/198	0.95 (0.71 to 1.27)	45/128	1.26 (0.89 to 1.79)	163/559	0.93 (0.78 to 1.12)
Tumor stage†								
T1	5/60	1.00 (reference)	5/94	1.00 (reference)	13/49	1.00 (reference)	23/203	1.00 (reference)
T2	47/216	2.86 (1.13 to 7.19)	57/223	3.68 (1.47 to 9.20)	35/166	1.16 (0.61 to 2.22)	139/605	2.08 (1.34 to 3.24)
T3	110/386	4.30 (1.74 to 10.63)	109/375	5.04 (2.04 to 12.42)	79/233	1.74 (0.94 to 3.24)	298/994	2.95 (1.92 to 4.54)
T4	81/177	7.65 (3.05 to 19.21)	90/166	9.37 (3.79 to 23.20)	50/116	3.46 (1.78 to 6.72)	221/459	5.42 (3.49 to 8.40)
Radiation technique								
2D-CRT	215/679	1.00 (reference)	214/541	1.00 (reference)	173/525	1.00 (reference)	602/1745	1.00 (reference)
IMRT	28/160	0.42 (0.28 to 0.64)	47/317	0.48 (0.34 to 0.66)	4/39	0.31 (0.11 to 0.86)	79/516	0.44 (0.34 to 0.56)
Treatment								
RT alone	58/248	1.00 (reference)	41/148	1.00 (reference)	55/215	1.00 (reference)	154/611	1.00 (reference)
RT+IC/AC	67/232	0.98 (0.67 to 1.43)	68/159	1.62 (1.09 to 2.42)	60/142	0.93 (0.61 to 1.41)	195/533	1.13 (0.90 to 1.41)
CCRT	118/359	1.01 (0.72 to 1.42)	152/551	1.15 (0.80 to 1.65)	62/207	0.86 (0.58 to 1.29)	332/1117	1.01 (0.83 to 1.24)

*Adjusted hazard ratios (HRs) and 95% CIs for TLI development were calculated by Cox proportional hazard model using variables including sex, age group, tumor stage, radiation technique, and treatment modality. CI = confidence interval; 2D-CRT = two-dimensional conformal radiotherapy; IMRT = intensity-modulated radiotherapy; RT = radiotherapy alone; RT+IC/AC = radiotherapy with induction and/or adjuvant chemotherapy; CCRT = concurrent chemoradiotherapy; TLI = temporal lobe injury.

†The patients were staged according to the 2002 6th UICC/AJCC staging system (22).

of *CEP128* associated with TLI development (Supplementary Table 3, available online). Two SNPs, rs17111237 and rs17111246, located within 2 kb upstream of *CEP128* (Figure 2B) were in nearly complete LD ($R^2 = 0.99$, Supplementary Figure 4, available online). The per-allele HR of the minor allele at rs17111237 was 1.63 (MAF = 0.13; 95% CI = 1.27 to 2.08; $P = 1.02 \times 10^{-4}$) (Table 2) and it showed moderate LD with the top signal rs162171 ($R^2 = 0.69$).

To confirm the above findings, we genotyped the identified SNPs in two stages, including 1119 NPC patients from GARTP study (2008–2010) and 741 NPC patients in 2002–2004 and in 2005–2007 (GARTP) (Figure 1 and Table 1). The average MRI follow-ups for patients in the first and the second replication stages are 4.98 and 3.01 times and the median follow-up months are 35.2 and 26.6, respectively. All the SNPs in *CEP128* were associated with TLI risk with *P* less than .05. When combining the patients from three stages, we found that patients carrying the minor alleles at rs162171 or rs17111237 tend to have higher risks to develop TLI with per allele HRs of 1.46 (MAF:0.18, 95% CI = 1.29 to 1.66, $P_{combined}=6.17 \times 10^{-9}$) and 1.45 (MAF:0.14, 95% CI = 1.26 to 1.66, $P_{combined}=3.18 \times 10^{-7}$), respectively (Table 2, Figure 2C and Supplementary Figure 5, available online). None in *KCTD1* or *DISC1FP1* reached the statistical significance level of *P* less than .05 in the replication analysis.

We further performed expression quantitative trait locus (eQTL) analysis and found that with the increasing number of risk alleles at rs162171 or rs17111237, *CEP128* exhibited a lower mRNA expression level in human lymphoblastoid cell line (Hapmap database: http://www.hapmap.org/) and intralobular white matter of human brain tissue (BRAINEAC database, http://www.braineac.org/) (Figure 3A,B). Furthermore, the results of dual-luciferase assay showed that the transcription activities of promoter constructs harboring the risk allele of rs17111237 and rs17111246 were lower than that of the wildtype constructs (Figure 3C), indicating that individuals harboring risk alleles might present an impaired expression level and insufficient function of *CEP128*.

Radiation-induced brain injury has been speculated as a multistep process, during which direct damage and vascular abnormality may disturb the balance of oxidative metabolism, which could activate the release of reactive oxygen species and generate deleterious oxidative stress. To further investigate the role of *CEP128* involved in radiation-induced brain injury, we imitated the direct radiation effect and oxidative stress effect on gliocytes by treating the glioblastoma cell line U87 with X-ray and H_2O_2. Our results of the clonogenic assay showed that RNAi inhibition of endogenous *CEP128* expression reduced the survival fraction of U87 cell lines under the treatment of X-ray (Figure 3D,E). Additionally, we found that after being treated with X-ray or H_2O_2, a higher level of cell death and apoptosis was observed in U87 cell lines with RNAi inhibition of endogenous *CEP128* expression, implicating a potential biological involvement of *CEP128* in protecting normal temporal lobes against radiation-induced damage (Supplementary Figures 6 and 7, available online).

To further evaluate the underlying disease mechanisms responsible for the genetic signals, we applied g:Profiler (29) and Gene-set Enrichment Analysis (GSEA) (30) to identify overrepresented pathways using SNPs located within 20 kb upstream/downstream of 212 candidate genes with $P < .001$ in the GWAS analysis. The top 20 enriched gene sets identified by g:Profiler

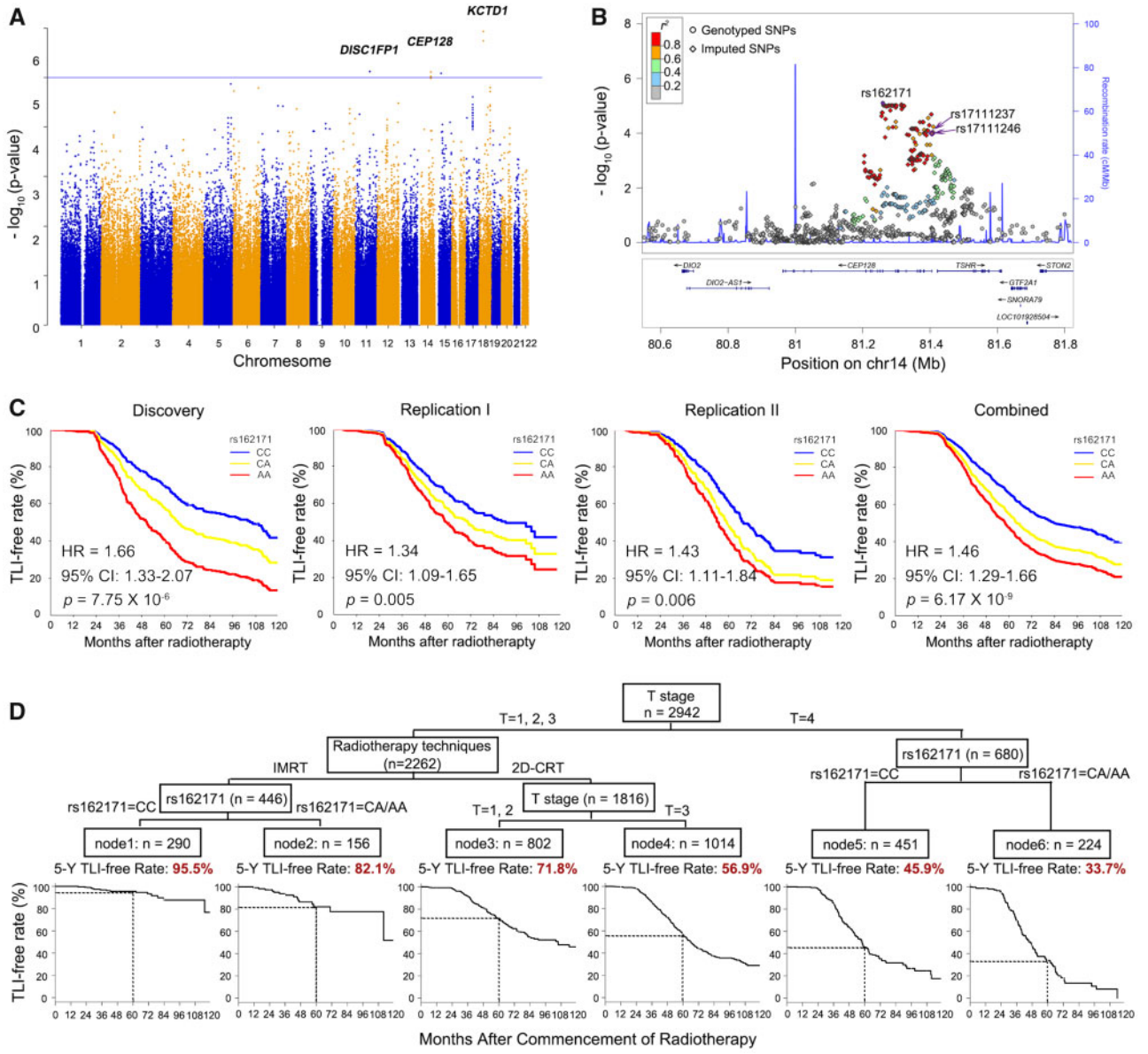

Figure 2. Genome-wide association results and the estimated curves of TLI development in different stages and subgroups. **A)** Genome-wide $-log_{10}$ *P* values from the survival analysis for 445 078 SNPs from the discovery stage are shown. The blue line represents $P = 1.0 \times 10^{-5}$. **B)** The $-log_{10}$ *P* values of the SNPs are shown according to their physical positions. The recombination rates (shown as blue lines) were estimated from the 1000 Genome ASN panel. The genotyped SNPs and the imputed SNPs are shown as circles and diamonds. The two variants rs17111237 and rs17111246 located within 2 kb upstream of *CEP128* are in purple outlines. **C)** The estimated curves of TLI development among patients carrying minor-allele homozygotes, heterozygotes, and major-allele homozygotes at rs162171. HRs and two-sided Wald test *P*-values were calculated using multivariate Cox proportional hazard regression models assuming additive effect of minor alleles and adjusting age at NPC diagnosis, tumor stage, and radiotherapy technique as covariates. **D)** The partition trees constructed using the combined samples from the three-stage. Each node was split by the indicated variable that has the best performance in partitioning the samples into two groups. The curves in the terminal nodes reflect the TLI development in different subgroups. T = tumor; IMRT = intensity-modulated radiotherapy; TLI = temporal lobe injury; HR = hazard ratio; CI = confidence interval.

and GSEA are listed in Supplementary Tables 4 and 5 (available online). "GO neurogenesis" (27 of 212 genes, 12.7%) was identified by both softwares (Supplementary Table 6, available online). In addition, the candidate genes were also clustered in the gene sets such as "immune system process", "programmed cell death", "generation of neurons", and "apoptotic process".

Based on our genetic findings, we further divided the patients into six subgroups by using the genetic and clinical variables (Figure 2D) (31). For patients in the T1–T3 classification, the radiation technique was chosen as the next variable, where patients in the IMRT group carrying CC genotype at rs162171 have the lowest TLI risk (5-year TL-free rate of 95.5%, 95% CI = 92.5 to 98.6%) and the risk elevated among those carrying the risk genotypes of rs162171 (5-year TLI-free rate of 82.1%, 95% CI = 73.2 to 92.0%). Unsurprisingly the patients in the T4 classification had the higher TLI risk. Among these patients, the ones who carried risk genotypes at rs162171 had the highest risk (5-year TLI-free rate of 33.7%, 95% CI = 25.6 to 44.4%). The resulting classification further indicated that the patients who have the same clinical characteristics could have varying TLI risk due to a different genetic background.

ARTICLE

Table 2. Associations of SNPs with development of temporal lobe injury after radiation in nasopharyngeal carcinoma patients

				AA*		AB*		BB*			
SNPs	Locus	Stage	MAF	N	TLI %	N	TLI %	N	TLI %	HR (95% CI)†	P†
rs162171	*CEP128*	Discovery	0.171	748	19.4%	297	29.3%	37	29.7%	1.66 (1.33 to 2.07)	7.75×10^{-6}
C/A‡	Intron	Replication I	0.194	714	22.0%	368	25.3%	32	34.4%	1.34 (1.09 to 1.65)	.005
		Replication II	0.180	491	21.0%	211	30.3%	25	32.0%	1.43 (1.11 to 1.84)	.006
		Combined	0.182	1953	20.7%	876	27.9%	94	31.9%	1.46 (1.29 to 1.66)	6.17×10^{-9}
rs17111237	*CEP128*	Discovery	0.131	788	20.4%	235	31.5%	19	21.1%	1.63 (1.27 to 2.08)	1.02×10^{-4}
A/G‡	Promoter	Replication I	0.138	823	22.8%	271	24.0%	18	38.9%	1.32 (1.05 to 1.66)	.02
		Replication II	0.143	544	21.9%	180	28.9%	16	37.5%	1.41 (1.07 to 1.84)	.01
		Combined	0.137	2155	21.7%	686	27.8%	53	32.1%	1.45 (1.26 to 1.66)	3.18×10^{-7}
rs9304497	*KCTD1*	Discovery	0.278	576	20.1%	409	23.7%	96	31.3%	1.60 (1.33 to 1.94)	1.19×10^{-6}
G/A‡	Intron	Replication I	0.269	605	22.2%	416	26.4%	91	17.6%	1.03 (0.85 to 1.25)	.77
		Replication II	0.298	376	24.5%	288	25.0%	77	16.9%	0.88 (0.70 to 1.11)	.29
		Combined	0.280	1557	22.0%	1113	25.1%	264	22.4%	1.19 (1.06 to 1.34)	.004
rs10501719	*DISC1FP1*	Discovery	0.111	850	21.2%	221	25.8%	9	66.7%	1.81 (1.40 to 2.35)	7.70×10^{-6}
A/G‡	Intron	Replication I	0.111	877	23.5%	222	22.5%	12	33.3%	1.00 (0.76 to 1.31)	.98
		Replication II	0.123	570	24.2%	159	23.9%	12	8.3%	0.97 (0.69 to 1.36)	.87
		Combined	0.114	2297	22.8%	602	24.1%	33	33.3%	1.24 (1.05 to 1.46)	.01

*Genotypes are shown as AA for major-allele homozygotes, AB for heterozygotes and BB for minor-allele homozygotes. SNP = single-nucleotide polymorphism; HR = hazard ratio; CI = confidence interval; TLI = temporal lobe injury; MAF: minor allele frequency.
†HRs, 95% CIs and two-sided Wald test P-values were calculated using multivariate Cox proportional hazard regression models assuming additive effect of minor alleles and adjusting age at NPC diagnosis, tumor stage, and radiotherapy technique as covariates.
‡The major allele/minor allele of the SNP.

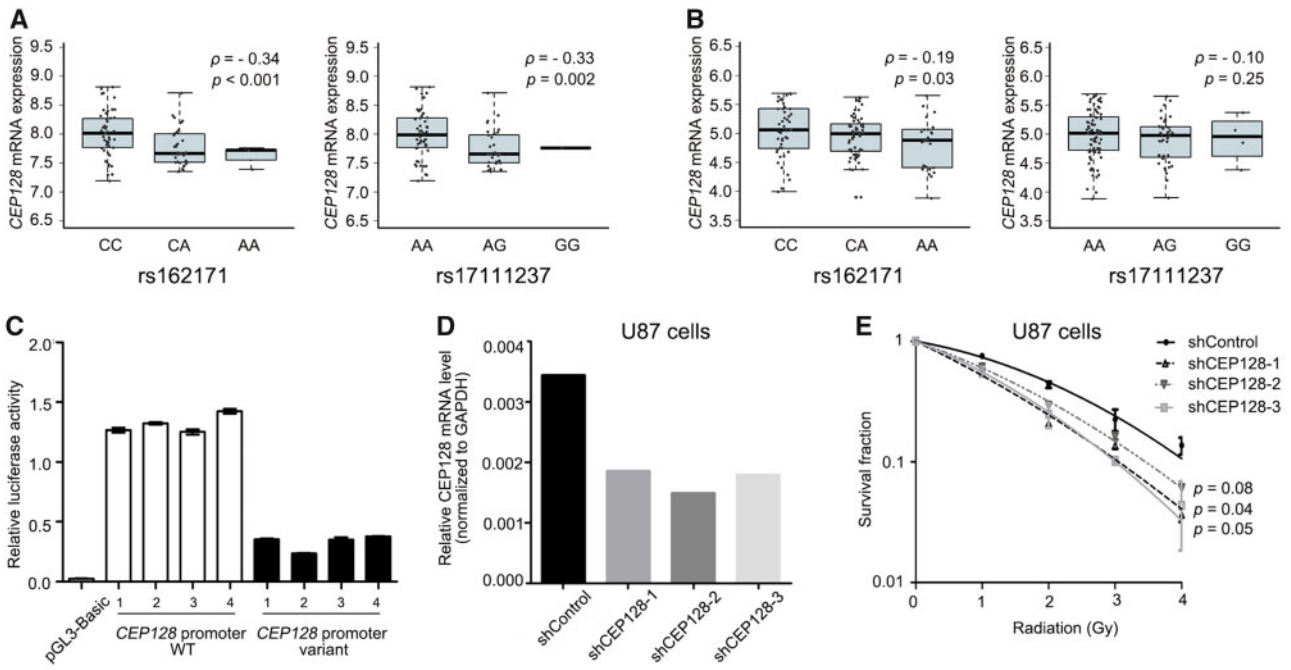

Figure 3. Expression quantitative trait locus (eQTL) analysis and functional characterizations of the protective role of *CEP128* gene in radiosensitivity. **A,B**) Visualization of association trends for rs162171, rs17111237, and *CEP128* mRNA expression in (**A**) HapMap CHB (Han Chinese in Beijing, China) and JPT (Japanese in Tokyo, Japan) and (**B**) in the intralobular white matter of human brain in the UK brain expression consortium (UKBEC). Gene expression values observed in each individual are shown by points. The correlation was represented by ρ and P values were calculated by Spearman correlation test. **C**) The means ± SD ($N = 3$) of luciferase activity detection. "*CEP128* promoter WT" means luciferase vector containing a segment of *CEP128* promoter with rs1711237A and rs1711246G, "*CEP128* promoter variant" means luciferase vector containing a segment of *CEP128* promoter with rs1711237G and rs1711246A. The numbers 1, 2, 3, 4 in the x-axis indicate four independent luciferase vectors. **D**) The means of relative mRNA expression levels ($N = 2$) of *CEP128* after stable inhibition of endogenous *CEP128* using shRNA in the U87 cell line. sh*CEP128*–1, 2, and 3 indicate three shRNAs targeting different regions of *CEP128* mRNA. **E**) The clonogenic survival curve was established on day 10 after stable transfected cells received indicated doses of radiation. Survival fractions were calculated. Data represent means ± SD ($N = 3$) and *P* values were calculated by two-sided *t*-test for shRNA vs sh-control.

ARTICLE

Discussion

In this prospective observational study, we identified genetic variants in a centrosomal protein *CEP128* that conferred the risk of radiation-induced TLI in NPC patients. We found that rs162171 in the intron of *CEP128* was statistically significantly associated with TLI development. Additionally, the A > G transition at rs17111237 in *CEP128* promoter may cause downregulation of this gene, which could further increase the radiosensitivity of glioblastoma cell lines, suggesting the protective role of *CEP128* against radiation toxicity in normal brain tissue.

CEP128 is a newly characterized centrosome protein (CEP) which is a key regulator of ciliation (32) and plays important roles in cell cycle progression (33). Increasing evidence has indicated that primary cilia plays important roles in coordinating a variety of cellular signaling pathways in neuronal cell and regulate cell migration, differentiation, as well as a host of adult behaviors (34). Functions of primary cilia can be dramatically affected by either the malfunction of ciliary genes or various external factors, including radiation. Interestingly, *CEP128* appears to associate with both the cilia function maintenance and radiation response of cells. Knockdown of *CEP128* could lead to abnormally high levels of ciliation in proliferating cells (35), and multiple *CEP128* interactors enriched by ciliogenesis induction, including *CASK*, *CEP72*, and *LMO7*, were associated with ionizing radiation (IR) resistance in a recent genome-wide RNAi screen study (36). Identification of genetic variants in an essential gene of primary cilia provides not only novel insights into the underlying mechanisms of radiation-induced brain injury, but also a new list of potential treatment targets to prevent or ameliorate the side effects of radiotherapy.

Cerebrovascular injury and remodeling is another suggested hypothesis on the development of radiation-induced brain injury. Evidence has shown the vascular structural and functional alteration after fractional whole-brain irradiation (fWBI) in rodents (37–39) and nonhuman primate (NHP) models (40–42). A recent NHP study reported white matter-specific transcriptional alterations of genes involving cerebrovascular remodeling, blood–brain barrier integrity, neurotransmission, and inflammation (42). Interestingly, we found 34 SNPs in these genes associated with TLI with *P* less than .01 in our samples (data not shown). More studies are warranted to further investigate the underlying mechanisms of vascular abnormality in the development of TLI.

Temporal lobe injury has generally been regarded as a progressive and irreversible complication in the radiotherapy of NPC (43). Although the TLI rate is decreasing in the NPC survivors in the era of IMRT, there is still 3.2–12.9% of NPC patients suffering TLI (5–9,44). Moreover, temporal lobe protection is arduous, particularly in patients with T4 disease, with higher injury rates up to 25.0% (6). Hence, pretreatment assessment and prevention of adverse responses is of critical importance. Some ongoing or completed preclinical studies (39,45,46) and clinical trials (47–50) have proven that clinical intervention could effectively treat or even reverse radiation-induced brain injury. Furthermore, the risk prediction integrating the genetic findings and clinical variables showed that those patients with high risks of TLI could be identified in advance, suggesting that applying genetic risk profiling to clinical intervention may have potential value to prevent severe complications and improve the quality of life of NPC patients. Further studies might be warranted to investigate the clinical models generalized to other cancers.

The main limitation of this study is that dosage parameters of the temporal lobes, which were reported as important factors for the development of TLI (51,52), were not available and these parameters were not adjusted in the analysis. We made some attempts to overcome this limitation. First, we collected the information on prescribed total dose, dose per fraction, and overall treatment time of the nasopharynx. However, no association was observed between the dosage parameters and the development of TLI. These results might be explained by the similarity of dose prescription received by all the patients. Second, we took radiation techniques and tumor stages as covariates, which may reflect the dosage–volume parameter of the temporal lobes to some extent. In the patients who received IMRT or who were in early tumor stages, a smaller volume of the temporal lobes would receive high-dose irradiation. Additionally, when the associations were stratified by tumor stages or radiation techniques, the genetic effect remained statistically significant (data not shown).

In conclusion, using genome-wide association analysis followed by two independent replications and functional studies, we identified *CEP128* as a susceptibility gene of TLI development in NPC patients. Additional studies on how the CEP proteins participate in radiation-induced brain injury are required. Moreover, normal tissue sensitivity to radiation exposure has been regarded as a complex, polygenic trait resulting from interactions of numerous genes in different cellular pathways (53,54). Therefore, further experiments are needed to confirm our findings or to identify other additional susceptibility loci, which could provide the basis of individualized radiation treatment for patients.

Funding

This work was supported by grants from the National Key Research and Development Program of China (2016YFC1302704), National Key Research and Development Program of China (2016YFC0902001), Sino-Sweden Joint Research Programme (81861138006), the Science and Technology Planning Project of Guangzhou, China (201804020094), the Special Support Program for High-level Professionals on Scientific and Technological Innovation of Guangdong Province, China (2014TX01R201), Health & Medical Collaborative Innovation Project of Guangzhou City, China (201604020003), the Key Project for International Cooperation and Exchange of the National Natural Science Foundation of China (81220108022), National Science Fund for Distinguished Young Scholars of China (81325018), National High Technology Research and Development Program of China (the 863 Program: 2012AA02A206), the Science and Technology Planning Project of Guangdong Province, China (2011B031800218), National Natural Science Foundation of China (81201747, 81372882 and 81572781), Natural Science Foundation of Guangdong Province, China (S2012040006323, 2014A030313023), and the Open Foundation of State Key Laboratory of Oncology in South China (HN2013–07).

Notes

Affiliations of authors: State Key Laboratory of Oncology in South China, Collaborative Innovation Center for Cancer Medicine, Guangdong Key Laboratory of Nasopharyngeal

ARTICLE

Carcinoma Diagnosis and Therapy, Sun Yat-sen University Cancer Center, Guangzhou, China (TMW, GPS, MYC, JBZ, YS, JH, WQX, XZL, SYH, XHZ, SDZ, YZH, HDQ, JXB, JM, WHJ); Department of Radiation Oncology, First Affiliated Hospital, Sun Yat-sen University, Guangzhou, China (GPS); Department of Nasopharyngeal Carcinoma (MYC) and Department of Radiation Oncology (YS, JM), Sun Yat-sen University Cancer Center, Guangzhou, China; Department of Pediatric Surgery, Guangzhou Institute of Pediatrics, Guangzhou Women and Children's Medical Center, Guangzhou Medical University, Guangzhou, China (JH); Unit on Statistical Genomics, Division of Intramural Research Programs, National Institute of Mental Health, National Institutes of Health, Bethesda, MD (YYS); Laboratory of Malaria and Vector Research, National Institute of Allergy and Infectious Diseases, National Institutes of Health, Rockville, MD (JM).

The funders had no role in the design of the study; the collection, analysis, or interpretation of the data; the writing of the article; or the decision to submit the article for publication. The raw data of this article have been uploaded to the Research Data Deposit (RDD) with an RDD number of RDDA2018000620.

Disclosures: The authors have no conflicts of interest to disclose.

Author Contributions: Dr Wei-Hua Jia supervised the study and had full access to all the data in the study. Guo-Ping Shen, Ming-Yuan Chen, and Ying Sun collected the clinical data and followed up the MRI for the diagnosis of TLI. Tong-Min Wang and Guo-Ping Shen analyzed and interpreted the data. Jiang-Bo Zhang designed and performed the functional experiments. Shao-Yi Huang performed functional experiments. Xi-Zhao Li, Wen-Qiong Xue, Xiao-Hui Zheng, Shao-Dan Zhang, and Ye-Zhu Hu collected the samples. Jing He, Hai-De Qin, and Jin-Xin Bei conducted statistical analysis. Wei-Hua Jia and Tong-Min Wang wrote the article. Jianbing Mu and Yin Yao Shugart gave critical revision of the article. Jianbing Mu, Yin Yao Shugart, and Jun Ma gave important consultation to this work.

References

1. Stone JB, DeAngelis LM. Cancer-treatment-induced neurotoxicity—focus on newer treatments. *Nat Rev Clin Oncol*. 2016;13(2):92–105.
2. Lee AW, Law SC, Ng SH, et al. Retrospective analysis of nasopharyngeal carcinoma treated during 1976-1985: late complications following megavoltage irradiation. *Br J Radiol*. 1992;65(778):918–928.
3. Wang YX, King AD, Zhou H, et al. Evolution of radiation-induced brain injury: MR imaging-based study. *Radiology*. 2010;254(1):210–218.
4. Zhou GQ, Yu XL, Chen M, et al. Radiation-induced temporal lobe injury for nasopharyngeal carcinoma: a comparison of intensity-modulated radiotherapy and conventional two-dimensional radiotherapy. *PLoS One*. 2013;8(7):e67488.
5. Jin YN, Zhang WJ, Cai XY, et al. The characteristics and survival outcomes in patients aged 70 years and older with nasopharyngeal carcinoma in the intensity-modulated radiotherapy era. *Cancer Res Treat*. 2018; doi: 10.4143/crt.2017:551.
6. Feng M, Huang Y, Fan X, et al. Prognostic variables for temporal lobe injury after intensity modulated-radiotherapy of nasopharyngeal carcinoma. *Cancer Med*. 2018;7(3):557–564.
7. Liyan L, Si W, Qian W, et al. Diffusion kurtosis as an in vivo imaging marker of early radiation-induced changes in radiation-induced temporal lobe necrosis in nasopharyngeal carcinoma patients. *Clin Neuroradiol*. 2017; doi: 10.1007/s00062-017-0585-9 [Epub ahead of print].
8. Liang SB, Wang Y, Hu XF, et al. Survival and toxicities of IMRT based on the RTOG protocols in patients with nasopharyngeal carcinoma from the endemic regions of China. *J Cancer*. 2017;8(18):3718–3724.
9. Kong C, Zhu XZ, Lee TF, et al. LASSO-based NTCP model for radiation-induced temporal lobe injury developing after intensity-modulated radiotherapy of nasopharyngeal carcinoma. *Sci Rep*. 2016;6(1):26378.
10. Lee AW, Ng SH, Ho JH, et al. Clinical diagnosis of late temporal lobe necrosis following radiation therapy for nasopharyngeal carcinoma. *Cancer*. 1988;61(8):1535–1542.
11. Lee AW, Foo W, Chappell R, et al. Effect of time, dose, and fractionation on temporal lobe necrosis following radiotherapy for nasopharyngeal carcinoma. *Int J Radiat Oncol Biol Phys*. 1998;40(1):35–42.
12. West CM, Barnett GC. Genetics and genomics of radiotherapy toxicity: towards prediction. *Genome Med*. 2011;3(8):52.
13. Kerns SL, Ostrer H, Rosenstein BS. Radiogenomics: using genetics to identify cancer patients at risk for development of adverse effects following radiotherapy. *Cancer Discov*. 2014;4(2):155–165.
14. Herskind C, Talbot CJ, Kerns SL, et al. Radiogenomics: a systems biology approach to understanding genetic risk factors for radiotherapy toxicity? *Cancer Lett*. 2016;382(1):95–109.
15. Ghazali N, Shaw RJ, Rogers SN, et al. Genomic determinants of normal tissue toxicity after radiotherapy for head and neck malignancy: a systematic review. *Oral Oncol*. 2012;48(11):1090–1100.
16. Kerns SL, Ostrer H, Stock R, et al. Genome-wide association study to identify single nucleotide polymorphisms (SNPs) associated with the development of erectile dysfunction in African-American men after radiotherapy for prostate cancer. *Int J Radiat Oncol Biol Phys*. 2010;78(5):1292–1300.
17. Kerns SL, Stock R, Stone N, et al. A 2-stage genome-wide association study to identify single nucleotide polymorphisms associated with development of erectile dysfunction following radiation therapy for prostate cancer. *Int J Radiat Oncol Biol Phys*. 2013;85(1):e21–e28.
18. Kerns SL, Stone NN, Stock RG, et al. A 2-stage genome-wide association study to identify single nucleotide polymorphisms associated with development of urinary symptoms after radiotherapy for prostate cancer. *J Urol*. 2013;190(1):102–108.
19. Kerns SL, Stock RG, Stone NN, et al. Genome-wide association study identifies a region on chromosome 11q14.3 associated with late rectal bleeding following radiation therapy for prostate cancer. *Radiother Oncol*. 2013;107(3):372–376.
20. Fachal L, Gomez-Caamano A, Barnett GC, et al. A three-stage genome-wide association study identifies a susceptibility locus for late radiotherapy toxicity at 2q24.1. *Nat Genet*. 2014;46(8):891–894.
21. Barnett GC, Thompson D, Fachal L, et al. A genome wide association study (GWAS) providing evidence of an association between common genetic variants and late radiotherapy toxicity. *Radiother Oncol*. 2014;111(2):178–185.
22. Greene FL, American Joint Committee on Cancer, American Cancer Society. *AJCC Cancer Staging Handbook: From the AJCC Cancer Staging Manual*. 6th ed. New York: Springer; 2002.
23. Sun Y, Zhou GQ, Qi ZY, et al. Radiation-induced temporal lobe injury after intensity modulated radiotherapy in nasopharyngeal carcinoma patients: a dose-volume-outcome analysis. *BMC Cancer*. 2013;13(1):397.
24. Andersen PK, Gill RD. Cox's regression model for counting processes a large sample study. *Ann Stat*. 1982;10(4):1100.
25. Devlin B, Roeder K. Genomic control for association studies. *Biometrics*. 1999;55(4):997–1004.
26. Andersen PK, Borch-Johnsen K, Deckert T, et al. A Cox regression model for the relative mortality and its application to diabetes mellitus survival data. *Biometrics*. 1985;41(4):921–932.
27. Kerns SL, de Ruysscher D, Andreassen CN, et al. STROGAR—Strengthening the reporting of genetic association studies in radiogenomics. *Radiother Oncol*. 2014;110(1):182–188.
28. Howie BN, Donnelly P, Marchini J. A flexible and accurate genotype imputation method for the next generation of genome-wide association studies. *PLoS Genet*. 2009;5(6):e1000529.
29. Reimand J, Arak T, Adler P, et al. g:profiler-a web server for functional interpretation of gene lists (2016 update). *Nucleic Acids Res*. 2016;44(W1):W83–W89.
30. Subramanian A, Tamayo P, Mootha VK, et al. Gene set enrichment analysis: a knowledge-based approach for interpreting genome-wide expression profiles. *Proc Natl Acad Sci USA*. 2005;102(43):15545–15550.
31. Hothorn T, Hornik K, Zeileis A. Unbiased recursive partitioning: a conditional inference framework. *J Comput Graph Stat*. 2006;15(3):651–674.
32. Monnich M, Borgeskov L, Breslin L, et al. CEP128 localizes to the subdistal appendages of the mother centriole and regulates TGF-beta/BMP signaling at the primary cilium. *Cell Rep*. 2018;22(10):2584–2592.
33. Kumar A, Rajendran V, Sethumadhavan R, et al. CEP proteins: the knights of centrosome dynasty. *Protoplasma*. 2013;250(5):965–983.
34. Guemez-Gamboa A, Coufal NG, Gleeson JG. Primary cilia in the developing and mature brain. *Neuron*. 2014;82(3):511–521.
35. Gupta GD, Coyaud E, Goncalves J, et al. A dynamic protein interaction landscape of the human centrosome-cilium interface. *Cell*. 2015;163(6):1484–1499.
36. Hurov KE, Cotta-Ramusino C, Elledge SJ. A genetic screen identifies the Triple T complex required for DNA damage signaling and ATM and ATR stability. *Genes Dev*. 2010;24(17):1939–1950.
37. Shi L, Linville MC, Iversen E, et al. Maintenance of white matter integrity in a rat model of radiation-induced cognitive impairment. *J Neurol Sci*. 2009;285(1–2):178–184.
38. Brown WR, Thore CR, Moody DM, et al. Vascular damage after fractionated whole-brain irradiation in rats. *Radiat Res*. 2005;164(5):662–668.
39. He F, Zou JT, Zhou QF, et al. Glatiramer acetate reverses cognitive deficits from cranial-irradiated rat by inducing hippocampal neurogenesis. *J Neuroimmunol*. 2014;271(1–2):1–7.

40. Caveness WF. Pathology of radiation damage to the normal brain of the monkey. *Natl Cancer Inst Monogr*. 1977;46:57–76.
41. Hanbury DB, Robbins ME, Bourland JD, et al. Pathology of fractionated whole-brain irradiation in rhesus monkeys (Macaca mulatta). *Radiat Res*. 2015;183(3):367–374.
42. Andrews RN, Metheny-Barlow LJ, Peiffer AM, et al. Cerebrovascular remodeling and neuroinflammation is a late effect of radiation-induced brain injury in non-human primates. Radiat *Res*. 2017;187(5):599–611.
43. Sheline GE, Wara WM, Smith V. Therapeutic irradiation and brain injury. *Int J Radiat Oncol Biol Phys*. 1980;6(9):1215–1228.
44. Takiar V, Ma D, Garden AS, et al. Disease control and toxicity outcomes for T4 carcinoma of the nasopharynx treated with intensity-modulated radiotherapy. *Head Neck*. 2016;38(S1):E925–E933.
45. Xu P, Xu Y, Hu B, et al. Extracellular ATP enhances radiation-induced brain injury through microglial activation and paracrine signaling via P2X7 receptor. *Brain Behav Immun*. 2015;50:87–100.
46. Jiang X, Engelbach JA, Yuan L, et al. Anti-VEGF antibodies mitigate the development of radiation necrosis in mouse brain. *Clin Cancer Res*. 2014;20(10):2695–2702.
47. Benoit A, Ducray F, Cartalat-Carel S, et al. Favorable outcome with bevacizumab after poor outcome with steroids in a patient with temporal lobe and brainstem radiation necrosis. *J Neurol*. 2011;258(2):328–329.
48. Levin VA, Bidaut L, Hou P, et al. Randomized double-blind placebo-controlled trial of bevacizumab therapy for radiation necrosis of the central nervous system. *Int J Radiat Oncol Biol Phys*. 2011;79(5):1487–1495.
49. Tang Y, Rong X, Hu W, et al. Effect of edaravone on radiation-induced brain necrosis in patients with nasopharyngeal carcinoma after radiotherapy: a randomized controlled trial. *J Neurooncol*. 2014;120(2):441–447.
50. Wang XS, Ying HM, He XY, et al. Treatment of cerebral radiation necrosis with nerve growth factor: a prospective, randomized, controlled phase II study. *Radiother Oncol*. 2016;120(1):69–75.
51. Hsiao KY, Yeh SA, Chang CC, et al. Cognitive function before and after intensity-modulated radiation therapy in patients with nasopharyngeal carcinoma: a prospective study. *Int J Radiat Oncol Biol Phys*. 2010;77(3):722–726.
52. Mao YP, Yin WJ, Guo R, et al. Dosimetric benefit to organs at risk following margin reductions in nasopharyngeal carcinoma treated with intensity-modulated radiation therapy. *Chin J Cancer*. 2015;34(3):189–197.
53. Chang-Claude J, Ambrosone CB, Lilla C, et al. Genetic polymorphisms in DNA repair and damage response genes and late normal tissue complications of radiotherapy for breast cancer. *Br J Cancer*. 2009;100(10):1680–1686.
54. Travis EL. Genetic susceptibility to late normal tissue injury. *Semin Radiat Oncol*. 2007;17(2):149–155.